Received: 20 April 2021 | Revised: 28 July 2021 | Accepted: 4 August 2021

DOI: 10.1111/mpp.13130

ORIGINAL ARTICLE

Molecular Plant Pathology WILEY

Functional validation of pathogenicity genes in rice sheath blight pathogen *Rhizoctonia solani* by a novel host-induced gene silencing system

Mei Zhao[1] | Chenjiaozi Wang[1] | Jun Wan[1] | Zanfeng Li[1] | Dilin Liu[2] | Naoki Yamamoto[3] | Erxun Zhou[1] | Canwei Shu[1]

[1]Guangdong Province Key Laboratory of Microbial Signals and Disease Control, Department of Plant Pathology, South China Agricultural University, Guangzhou, China

[2]Guangdong Provincial Key Laboratory of New Technology in Rice Breeding, Guangzhou, China

[3]College of Agronomy, Sichuan Agricultural University, Chengdu, China

Correspondence
Canwei Shu, Guangdong Province Key Laboratory of Microbial Signals and Disease Control, Department of Plant Pathology, South China Agricultural University, Guangzhou, Guangdong, 510642, China.
Emails: shucanwei@scau.edu.cn (C.S.); 80053@sicau.edu.cn (N.Y.); exzhou@scau.edu.cn (E.Z.)

Funding information
The National Natural Science Foundation of China, Grant/Award Number: 31801677; The Major Program of Guangdong Basic and Applied Basic Research, Grant/Award Number: 2019B030302006; The Project by the Research Fund Program of Guangdong Provincial Key Laboratory of New Technology in Rice Breeding, Grant/Award Number: 2017B030314173

Abstract

Rice sheath blight, caused by the soilborne fungus *Rhizoctonia solani*, causes severe yield losses worldwide. Elucidation of the pathogenic mechanism of *R. solani* is highly desired. However, the lack of a stable genetic transformation system has made it challenging to examine genes' functions in this fungus. Here, we present functional validation of pathogenicity genes in the rice sheath blight pathogen *R. solani* by a newly established tobacco rattle virus (TRV)–host-induced gene silencing (HIGS) system using the virulent *R. solani* AG-1 IA strain GD-118. RNA interference constructs of 33 candidate pathogenicity genes were infiltrated into *Nicotiana benthamiana* leaves with the TRV-HIGS system. Of these constructs, 29 resulted in a significant reduction in necrosis caused by GD-118 infection. For further validation of one of the positive genes, *trehalose-6-phosphate phosphatase* (*Rstps2*), stable rice transformants harbouring the double-stranded RNA (dsRNA) construct for *Rstps2* were created. The transformants exhibited reduced gene expression of *Rstps2*, virulence, and trehalose accumulation in GD-118. We showed that the dsRNA for *Rstps2* was taken up by GD-118 mycelia and sclerotial differentiation of GD-118 was inhibited. These findings offer gene identification opportunities for the rice sheath blight pathogen and a theoretical basis for controlling this disease by spray-induced gene silencing.

KEYWORDS

rice disease control strategy, host-induced gene silencing, pathogenicity gene, *Rhizoctonia solani*, rice sheath blight

1 | INTRODUCTION

Rice (*Oryza sativa*) is one of the most important cereal crops cultivated around the world. Rice cultivation often suffers from several types of diseases, including rice sheath blight (RSB), caused by the basidiomycete fungus *Rhizoctonia solani*. RSB is one of the most devastating rice fungal diseases globally and causes significant yield losses and reductions in rice grain quality (Moni et al., 2016; Rao et al., 2019; Wang et al., 2018). RSB often occurs under warm and humid conditions, particularly in tropical areas. In China, RSB affects over 17 million hectares per year and results in a yield reduction as high as 50% in severely affected areas (https://www.natesc.org.cn).

R. solani exhibits a broad host range and causes catastrophic diseases in numerous plant species, including Asteraceae, Brassicaceae, Fabaceae, Poaceae, and Solanaceae, as well as some woody ornamental plants and forest trees (Ghosh et al., 2014; Pan et al., 1999; Zou et al., 2000). In nature, *R. solani* produces no asexual spores and exists mainly on crop residues and in the soil in the form of mycelia and sclerotia (Shu et al., 2019). Unfortunately, the molecular basis for RSB pathogenesis and rice–*Rhizoctonia* interaction is largely unknown (Molla et al., 2020), mainly due to the lack of rice cultivars with stable and perfect resistance to RSB and of efficient techniques for functional analysis of *R. solani* genes (Singh et al., 2019). Due to the broad host range, high genetic variability, and survival as sclerotia (Taheri & Tarighi, 2011; Tiwari et al., 2017; Yellareddygari et al., 2014; Zhu et al., 2019), farmers heavily rely on the use of chemical fungicides such as ARMURE and jinggangmycin (validamycin) to control RSB. However, excessive use of chemical fungicides may cause environmental pollution and increase the risk of fungicide resistance in the RSB pathogen (Singh et al., 2019).

In the last decades, elucidation of the pathogenic mechanism of the RSB pathogen has been accelerated thanks to de novo genome sequencing and transcriptome sequencing efforts (Singh et al., 2019; Zheng et al., 2013). In the earliest stage of RSB pathogenesis, sclerotia in the soil germinate to produce hyphae and attach to plants' surfaces. With the continuous branching, the hyphae gather to form infection cushions and penetrate rice cells or tissues (Taheri & Tarighi, 2011). Finally, water-soaked lesions develop and expand on rice sheath tissues. During the infection process, *R. solani* produces cell wall-degrading enzymes (e.g., pectinase, laccase, and xylanase) and some metabolites, including phytotoxins, facilitating its penetration into and killing of host cells (Rao et al., 2019; Singh & Subramanian, 2017; Yang et al., 2011). In recent years, three polygalacturonase (PG) genes, *Rrspg1*, *RsPG3*, and *RsPG4*, have been reported to induce tissue necrosis in rice sheath as essential virulence genes in the host–pathogen interaction (Chen et al., 2018; Yang et al., 2012). Recent studies reported effector-like proteins based on necrosis induction or cell death signalling in plant cells (Li et al., 2019; Yamamoto et al., 2019; Zheng et al., 2013). However, few pathogenicity genes have been identified in *R. solani*.

RNA interference (RNAi), or gene silencing, which is characterized by targeted mRNA degradation by the introduction of sequence-specific double-stranded RNA (dsRNA) into cells, has become an essential tool for studying gene functions (Kuo & Falk, 2020). Small interfering RNA duplexes (siRNAs) are derived from the processing of the dsRNA by an RNase III-like enzyme. Then siRNAs are recruited into a multiprotein complex known as RNA-induced silencing complex, which interacts with the target RNA to mediate cleavage in a catalytic fashion (Weiberg et al., 2015). Virus-induced gene silencing (VIGS) is a particular specific gene-silencing phenomenon triggered by dsRNA. It has been applied in examining gene functions in plants and adapted for high-throughput functional genomics (Su et al., 2020). Tobacco rattle virus (TRV), a bipartite virus, has been chiefly used as a vector in VIGS. In this case, pTRV1 encodes the replication and viral movement proteins, and pTRV2 encodes the coat protein and harbours the sequence used for VIGS. Inoculation of *Nicotiana benthamiana* with two different *Agrobacterium tumefaciens* strains, carrying pTRV1 and pTRV2, results in gene silencing (Robertson, 2004).

The exploration of mechanisms of cross-kingdom RNAi in the virulence and pathogenesis of pathogens, as well as host resistance, could significantly enhance our understanding of the *R. solani*–rice pathosystem. In 2010, Nowara et al. (2010) silenced *GTF1* and *GTF2* in the wheat and barley powdery mildew pathogen *Blumeria graminis* using the virus-induced gene silencing (VIGS) system with barley stripe mosaic virus (BSMV), which ultimately enhanced resistance in barley. From then on, a new procedure to determine the gene function of microbes by VIGS was proposed, and a new concept of host-induced gene silencing (HIGS) was put forward (Nowara et al., 2010). HIGS is an RNAi-based strategy that includes expressing a suitable RNAi structure in the host plant, targeting pathogen pathogenicity-related genes, and transferring dsRNA or siRNA into the pathogen during the interaction, followed by silencing of the target gene and suppression of virulence of the pathogen (Song & Thomma, 2016). The HIGS technique has been widely used in the study of biotrophic and necrotrophic fungi, including *Puccinia striiformis* (Zhu et al., 2017), *Verticillium dahliae* (Su et al., 2018; Su et al., 2017), and *Colletotrichum gloeosporioides* (Mahto et al., 2020).

RSB resistance is believed to be a quantitative trait that is under the control of many genes. To our knowledge, there are only two examples that showed increased RSB resistance by silencing pathogenicity genes of *R. solani* via stable rice transformation (Rao et al., 2019; Tiwari et al., 2017). To improve our understanding of the pathogenic mechanism of the RSB pathogen, in the present study we established a rapid and stable HIGS screening system for the identification of pathogenicity genes in the RSB fungus using the virulent *R. solani* AG-1 IA strain GD-118, which is also virulent to *N. benthamiana*. We showed reduced virulence of GD-118 to tobacco subjected to HIGS of 29 candidate pathogenicity genes. Stable rice transformation of siRNA targeting a *trehalose 6-phosphate phosphatase* gene of *R. solani* (*Rstps2*) increased resistance to RSB. This observation seemed to be attributable to the uptake of dsRNA of *Rstps2* by *R. solani* cells, resulting in a reduction of trehalose biosynthesis. Thus, we demonstrated that the HIGS system can be used to identify virulence factors in *R. solani*.

2 | RESULTS

2.1 | Screening of candidate pathogenic genes in *R. solani* AG-1 IA

We conducted a knowledge-based screening of candidate pathogenicity genes from the *R. solani* AG-1 IA reference genome (Zheng et al., 2013). All the predicted protein sequences were searched against the Pathogen-Host Interaction Database (PHI-base) (Urban et al., 2017) and the carbohydrate-active enzyme (CAZyme) database CAZy (Cantarel et al., 2009) to screen candidate pathogenicity genes. After compilation, 33 genes involved in diverse biological

processes (energy metabolism, development, protein secretion, and others) were selected for a functional test (Table S1). Gene expression patterns of these genes in *R. solani* AG-1 IA were clustered into four groups based on transcriptome data (Zheng et al., 2013) (Figure S1). Group A comprised genes showing the highest expression levels at 32 to 72 hr after inoculation (hai) of the pathogen. This group contained three genes encoding enzymes involved in trehalose metabolism. Group B contained genes showing the highest gene expression levels at 18 or 24 hai. Two *CAZyme* genes (*AG1IA_00742* and *AG1IA_01403*) were included in this group. Group C comprised genes showing the highest expression levels at 24 or 32 hai. This group contained two genes encoding capsular-associated proteins (*AG1IA_03049* and *AG1IA_03050*). Group D comprised genes showing the highest gene expression levels at 10 hai. It had two *CAZyme* genes (*AG1IA_01330* and *AG1IA_00669*). These results supported the reliability of our gene annotation-based selection of candidate pathogenicity genes. No significant sequence similarity was found between these candidate genes and internal genes in *N. benthamiana*. No possible off-target effect for the quantitative PCR (qPCR) primers was validated by SI-FI software (http://labtools.ipk-gatersleben.de/).

2.2 | Functional test of the candidate genes by TRV-HIGS

In this study, 35 *Agrobacterium* constructs, including a positive control construct pTRV2::*PDS*, a negative control construct pTRV2::*GFP* (RNAi-0), and 33 candidate gene constructs pTRV2::[RNAi-(1–33)], were agro-infiltrated into *N. benthamiana* leaves. Infiltration of pTRV2::*PDS* caused photobleaching at 10 days postinfiltration (dpi) (Figure S1a). Bleaching leaves appeared on the top of *N. benthamiana* initially and gradually expanded onto the whole plant until up to 20 dpi (Figure S2a). By contrast, infiltration of RNAi-0 produced no photobleaching (data not shown). These results indicated the appropriateness of our gene silencing system. The infiltrated tobacco with RNAi-0 allowed the growth of *R. solani* AG-1 IA strain GD-118 mycelia at 1 dpi and exhibited necrotic spots at 2 dpi (Figure S2b). After 5 days, almost all leaves withered, wilted, and tended to die (Figure S2b). By contrast, infiltrated tobacco plants with all candidate gene constructs exhibited lower disease index (DI) values than RNAi-0 tobacco plants but varied among each other (Figure 1). The DI value of RNAi-0 plants at 5 dpi was 86.11, while those of RNAi-(1–33) plants ranged from 22.22 to 69.44. Four RNAi constructs did not significantly reduce pathogenicity of GD-118 (Figure 1). These results suggested that 29 of the 33 candidate genes are involved in the pathogenic fitness of *R. solani*.

2.3 | Validation of the transient silencing effect of *Rstps2* on pathogenicity of *R. solani*

To validate the effect of silencing *AG1IA-04214* (RNAi-25), which targets a gene that encodes a trehalose 6-phosphate phosphatase (*Rstps2*), the tobacco plants transiently expressing pTRV:*Rstps2*

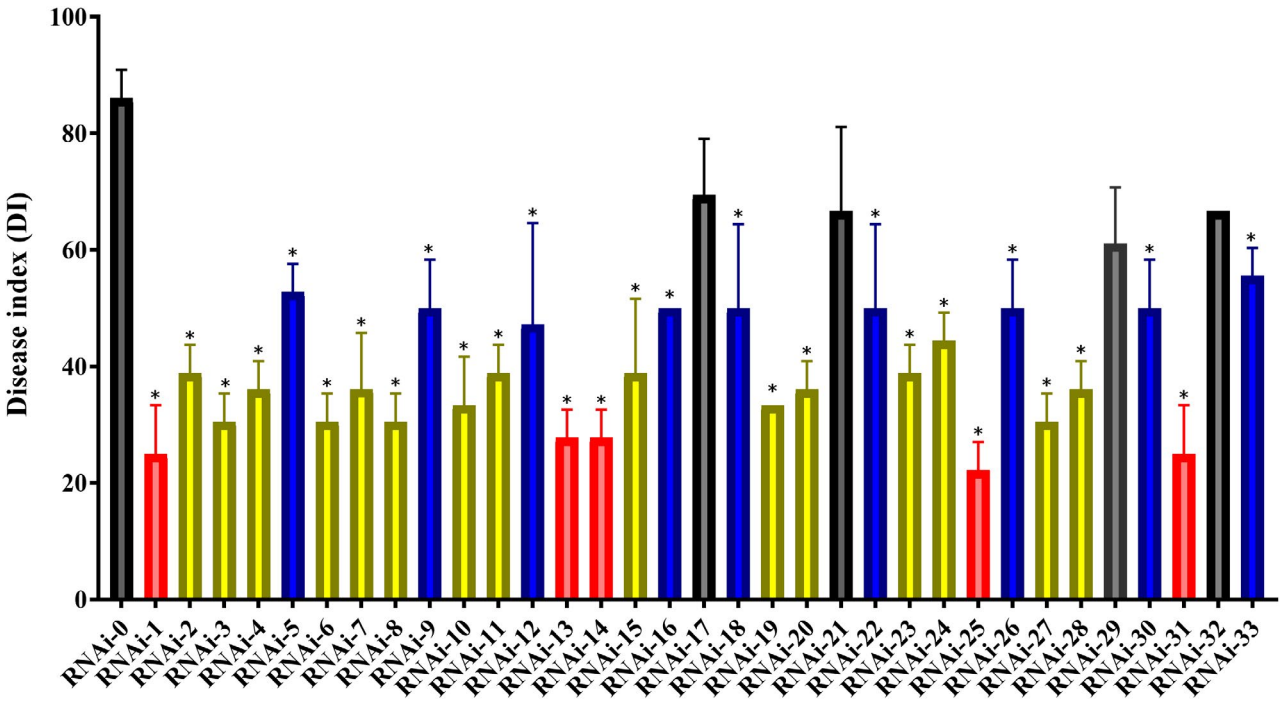

FIGURE 1 Disease index values in host-induced gene silencing (HIGS) assays in *Nicotiana benthamiana* for 33 candidate pathogenicity genes in *Rhizoctonia solani*. Highly resistant lines, moderately resistant lines, and slightly resistant lines are highlighted in red, blue, and yellow, respectively. Error bars represent standard errors of biological triplicates. $^{*}p < .05$, one-way analysis of variance with Tukey's post hoc test

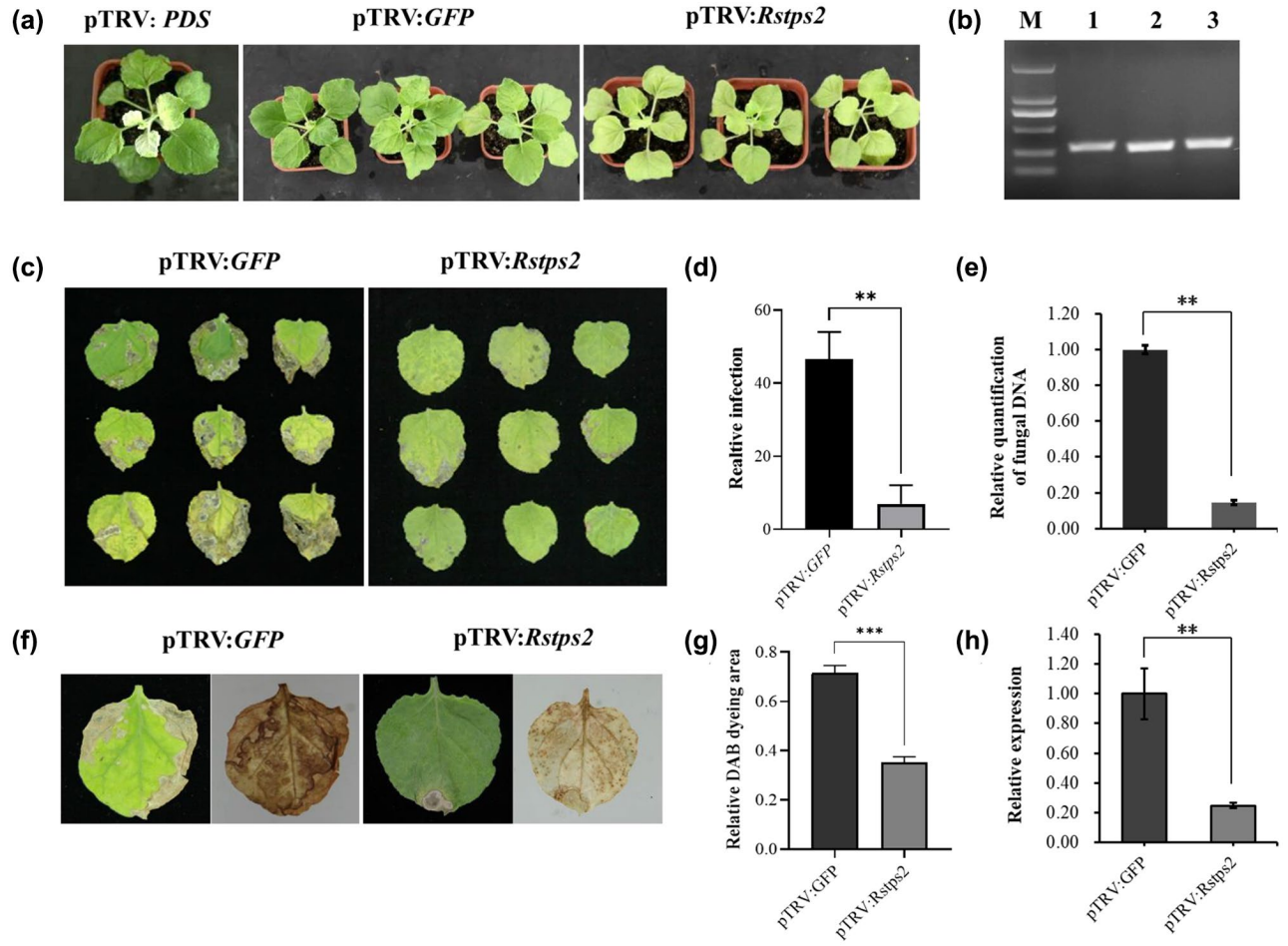

FIGURE 2 The effects of host-induced gene silencing (HIGS) for *Rstps2* on *Nicotiana benthamiana*. (a) The phenotype of pTRV2::*Rstps2*-infiltrated plants at 14 days after infiltration. (b) Reverse transcription PCR was used to monitor the expression levels of target genes in infiltrated plants. M: 2-kb DNA ladder; 1: pTRV2::*GFP*; 2: pTRV2::*PDS*; 3: pTRV2::*Rstps2*. (c) Necrotic symptoms on leaves inoculated with GD-118 at 5 days postinoculation (dpi). (d) Relative leaf area that was visibly infected at 5 dpi. (e) Relative amounts of GD-118 DNA. Fungal biomass was measured by quantitative PCR and normalized to *EF1α* transcript levels of *N. benthamiana*. (f) Reactive oxygen species detection by 3,3′-diaminobenzidine (DAB) staining in tobacco leaves. (g) Quantified leaf areas with brown spots by DAB staining. (h) Gene expression levels of *Rstps2*. The data were normalized to the *GAPDH* transcript levels of GD-118. Error bars represent *SE* ($n = 3$). $^{**}p < .01$, $^{***}p < .001$, Student's *t* test

were further characterized. The tobacco plants silenced for *Rstps2* exhibited no noticeable phenotypic difference to those of the negative control (Figure 2a). Reverse transcription (RT)-PCR assays were used to detect transcript levels of the targeted genes *Rstps2*, *GFP*, and *PDS* (Figure 2b). The agro-infiltrated tobacco silenced for *Rstps2* exhibited more resistance to GD-118 than the green fluorescent protein (GFP) control (Figure 2c). The increased resistance in *Rstps2*-infiltrated tobacco was supported by the decrease of visibly infected leaf area (Figure 2d), lower amount of biomass of the pathogen (Figure 2e), and smaller leaf area with reactive oxygen species (ROS) accumulation (Figure 2f). The relative infection area of *GFP* plants was 47.0% but that of *Rstps2* plants was 6.02% ($p < .01$; Figure 2d). Compared with *GFP* plants the fungal biomass of *Rstps2* plants decreased by 86% ($p < .01$; Figure 2e). The leaf area stained with 3,3′-diaminobenzidine (DAB) in *Rstps2* plants was less than half of that of *GFP* plants ($p < .001$; Figure 2g). As expected, the expression level of *Rstps2* plants was significantly lower (24.8%) than that of *GFP* plants (Figure 2h). These results indicated that silencing of *Rstps2* in GD-118 by the TRV-HIGS technique in *N. benthamiana* decreased virulence and inhibited mycelial growth.

Noteworthily, ROS accumulation was observed throughout the leaves of *Rstps2* plants. In *GFP* plants, severe disease symptoms appeared on the leaves' edges, and ROS was detected throughout the whole leaf (Figure 2f). By contrast, the *Rstps2* plant leaves had no prominent disease spots. The accumulation of ROS was observed as uniformly distributed spots over the whole leaf, indicating that GD-118 colonized the leaf successfully. These results indicated that the virulence of strain GD-118 decreased by transient silencing of *Rstps2* in *N. benthamiana* and that *N. benthamiana* generated moderate amounts of ROS to prevent further invasion of the pathogen.

2.4 | HIGS of *Rstps2* by stable transformation in rice

Validation of putative transgenic rice lines (T_0 generation) was conducted by detecting *Rstps2* and the selection marker *hygromycin resistance gene* (*hyg*) using genomic PCR with gene-specific primers (Table S2). Among 14 lines with hygromycin resistance, 11 lines were positive for both genes (Figure S4a). Three randomly selected T_0 generation rice plants exhibited more resistance against GD-118 than nontransformants, as determined by detached leaf assays (Figures S4b–d and S5a–d). In three of these T_0 lines with confirmed transgene integration by genomic Southern blot (Figure S4e), the fungal biomass decreased with statistical significance (Figure S4d). We used this line (named TPS-3) for further verification.

To check the inheritance of the increased resistance to GD-118, we analysed two T_2 transgenic lines, TPS-3-2 and TPS-3-6, which were derived from TPS-3. These T_2 lines harboured *hyg* and *Rstps2* genes and exhibited no differences in rice plant height and the number of effective tillers between the RNAi lines and nontransformants (Figure 3a–d). Genomic DNA Southern blot indicated stable inheritance of the transfer DNA (T-DNA) into the T_2 generation (Figure 3e). No obvious morphological abnormalities were observed in the RNAi transgenic rice lines (data not shown). We observed increased resistance to GD-118 in these T_2 rice lines as well (Figure 4a). Only a few mycelia and disease spots were observed in homozygous T_2 transgenic detached rice leaves at 60 and 120 hpi, respectively, whereas dense disease spots were observed in the wild-type (WT) rice leaves. The mycelial growth and fungal biomass significantly decreased. The relative infection area in T_2 transgenic rice lines was 9.34%, which was significantly reduced when compared with the WT (59.45%) at 5 dpi (Figure 4b,c). Intact rice plants grown in pots were used to confirm the increased resistance to GD-118 in the T_2 transgenic plants. Disease symptom development was less severe in the transgenic rice lines, and the height of exhibited disease spots in nontransformants was higher than in homozygous T_2 transgenic plants at 10 dpi (Figure 4d,e). Inheritance of increased resistance to GD-118 was observed in detached leaves of T_3 rice lines derived from T_2 Tps-3-2 and Tps-3-6 (Figure S6). These results indicated stable inheritance of silencing of *Rstps2* and increased RSB resistance, although the results are based only on one transgenic line.

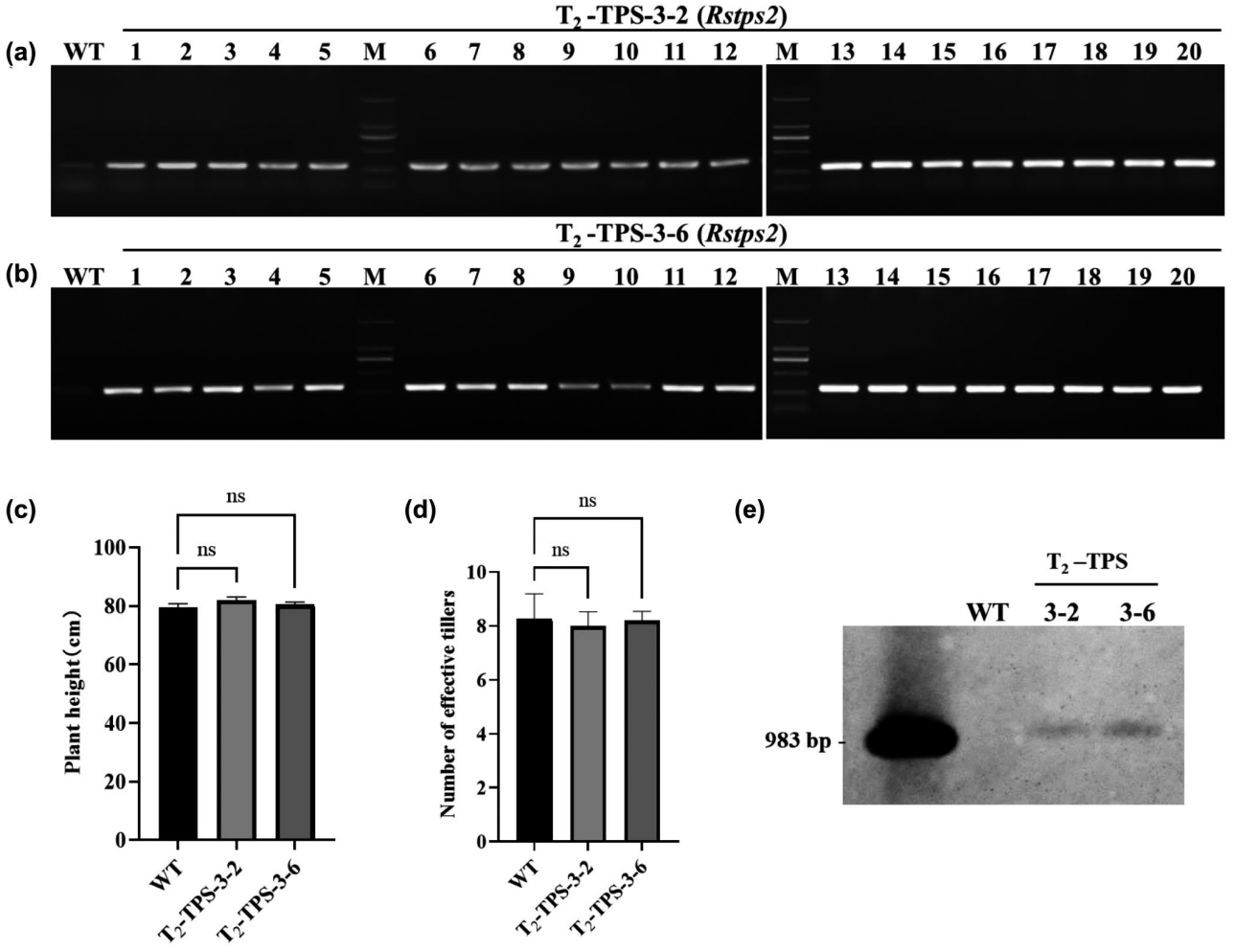

FIGURE 3 Molecular analysis and morphological characteristics of homozygous T_2 transgenic rice. (a,b) PCR analysis of T_2 transgenic plants using *Rstps2* gene-specific primers. (c) Plant height. (d) Number of tillers. (e) Southern blot analysis showing the integration of the transgene in the T_2-Tps2 lines. Data are shown as the mean ± *SE* of triplicates. ns: no significant changes observed, one-way analysis of variance and Tukey's test

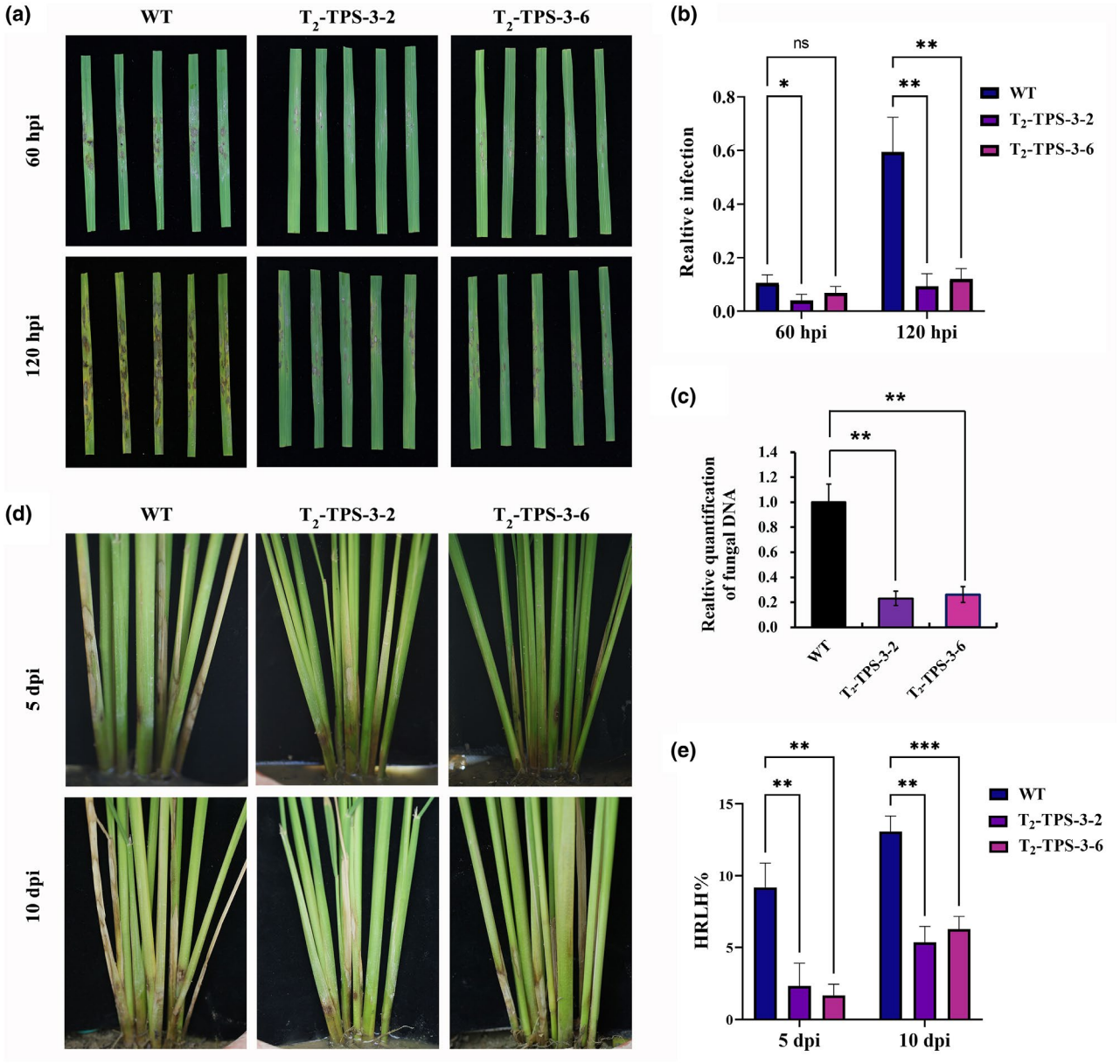

FIGURE 4 Evaluation of homozygous T_2 transgenic rice lines against the rice sheath blight pathogen *Rhizoctonia solani*. (a) Disease symptoms in *R. solani*-infected detached leaves of T_2 homozygous transgenic lines at 60 and 120 hr postinoculation (hpi). (b) Quantification of the visibly infected area at 60 and 120 hpi shown as the percentage of the total leaf area. $^{*}p < .05$, $^{**}p < .01$, two-way analysis of variance and Tukey's test. (c) Relative amounts of fungal DNA at 120 hpi as determined by quantitative PCR. The data were normalized to the 18S rRNA gene transcript levels of rice and are shown as the mean ± *SE* of triplicates. $^{**}p < .01$, one-way analysis of variance and Tukey's test. (d) Inoculation of plants by placing *R. solani* sclerotia in sheath tissue. (e) Highest relative lesion height (HRLH) in T_2 transgenic and nontransgenic (WT) controls at 5 and 10 days postinoculation (dpi). $^{**}p < .01$,$^{***}p < .001$, two-way analysis of variance Tukey's test [Correction added on 02 September 2021, after first online publication: Figure 4 has been updated in this version.]

2.5 | Concomitancy among silencing of *Rstps2*, reduced trehalose content, and increased levels of siRNA for *Rstps2* in GD-118 mycelia grown on HIGS rice

Trehalose 6-phosphate phosphatase (EC: 3.1.3.12) catalyses the reaction from trehalose 6-phosphate to trehalose, the last biochemical step in trehalose biosynthesis. We assumed that transformation of the RNAi construct for *Rstps2* led to an accumulation of siRNA for *Tps2*, silencing of *Tps2*, and inhibition of trehalose biosynthesis in GD-118 inoculated on the transgenic rice. As expected, the trehalose content in *R. solani*-(TPS-3-2) and *R. solani*-(TPS-3-6) was decreased by 31.17% and 34.61% when compared with the *R. solani*-(WT), respectively (Figure 5a). To test the persistence of siRNA, we subcultured the *R. solani*-(Tps-3-2) every 3 days as one generation (G). The transcript levels of *Rstps2* in G1 to G5 were significantly down-regulated by 9.20% to 60.43% compared with the nontransformants. There was no significant difference in *Rstps2* transcript levels between G1

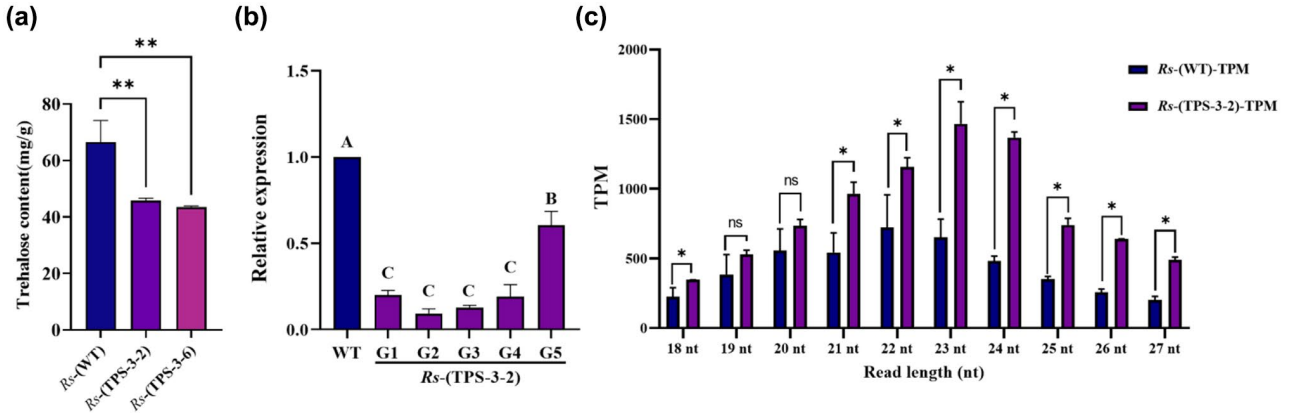

FIGURE 5 siRNA targeting *Rstps2* contributes to gene silencing and virulence inhibition. (a) The trehalose content of *Rhizoctonia solani*-(TPS-3-2/6) was significantly decreased. Data are shown as the mean ± *SE* of triplicates. $^{**}p < .01$, one-way analysis of variance (ANOVA) and Tukey's test. (b) Relative gene expression of *Rstps2* in standardized subcultured *R. solani*-(TPS-3-2). G1–G5: generation 1 to generation 5. The data were normalized to the *GAPDH* transcript levels of GD-118 and are shown as the mean ± *SE* of triplicates. Different labels represent statistical significance ($p < .01$), one-way ANOVA and Tukey's test. (c) Each read length transcripts per million (TPM) sum of *Rstps2*-derived specific siRNAs is the sum of all the TPM values of that read length. Data are shown as the mean ± *SE* of triplicates. Error bars represent *SE* ($n = 3$). $^{*}p < .05$, Student's *t* test

to G4, but there was a significant increase in G5 ($p < .001$). This result indicated that the effect of RNAi can continuously affect gene expression, leading to gene down-regulation. However, the effect of gene silencing decreased with multiple subgenerations (Figure 5b). For siRNA, we observed a significant increase of *Rstps2*-associated reads in small RNA sequencing (Figure 5c). The length distributions of siRNAs looked shifted to increased length (from 22 nucleotides [nt] in a nontransformant to 23 nt in the transgenic line). These results support the mechanistic view that siRNAs derived from *Rstps2* can enter pathogenic fungi from plants and silence the target gene to improve host resistance.

2.6 | Supplementation of exogenous dsRNA for *Rstps2* affects the expression of *Rstps2*

To further verify the mechanism of our HIGS technique in *R. solani*, we examined the effects of externally supplemented dsRNA for *Rspts2* on GD-118 cells. Coincubation of GD-118 mycelia with the dsRNAs reduced the gene expression levels of *Rstps2*. We observed 56.70%, 67.19%, 78.75%, and 83.69% reductions at 24, 48, 72, and 96 hr, respectively. There was no significant difference between 24, 48, 72, and 96 hr. The gene expression changes could be due to the result of the trafficking of the dsRNAs (Figure 6a). The mycelial growth rate and colony morphology of GD-118 showed no significant difference when grown on potato dextrose agar (PDA) plates (control) and PDA plates with dsRNA (500 ng/ml) (data not shown), but our study found that sclerotial differentiation was inhibited on PDA plates with dsRNA by 17.73% compared to controls (Figure 6b). We validated this by fluorescence microscopy (Figure 6c). A stronger fluorescence signal was observed in the hyphae at 24 hr, indicating GD-118 mycelia absorbed and/or adsorbed the labelled dsRNA from the medium. Thus, these results show a potential application of spray-induced gene silencing (SIGS) for biocontrol of *R. solani*.

3 | DISCUSSION

To date, HIGS has been reported in many important plant diseases caused by fungi and oomycetes, including *Puccinia striiformis*, *Puccinia triticina*, *Verticillium dahliae*, *Bremia lactucae*, *Phytophthora parasitica*, and *Phytophthora infestans* (Govindarajulu et al., 2015; Panwar et al., 2013; Sanju et al., 2015; Yin et al., 2011; Zhang et al., 2011, 2016). In this paper, we report an application of HIGS in *R. solani*, for which no genetic transformation techniques are available. Our HIGS system using *N. benthamiana* and GD-118 offers a relatively high-throughput experimental scheme with potential usefulness in other transformable plant species. At least, we demonstrated that the HIGS system is applicable to rice, which cannot undergo agro-infiltration-based VIGS. The TRV-HIGS system takes only 5–6 weeks to analyse the effect of silencing of pathogenicity gene candidates. Thus, the establishment of this HIGS system could accelerate functional validation of candidate pathogenicity genes and elucidation of the pathogenic mechanisms of *R. solani* diseases such as sheath blight and foliar blight.

In recent years, cross-pathogenicity of *R. solani* in *N. benthamiana* has been recognized, although tobacco plants were thought to be nonhost plants in nature (Anderson et al., 2016; Gonzalez et al., 2011). In our previous trials, we inoculated mycelial plugs or sclerotia to the stem base of *N. benthamiana*. This method resulted in propagation of mycelia and stem rot disease, but was not suitable for quantitative phenotyping of disease status (data not shown). Hence, in the present study, we sprayed a mycelial fragment suspension of GD-118 onto *N. benthamiana* using a spray bottle. This method allowed the observation of many disease spots with ROS accumulation on *N. benthamiana* leaves. Finally, we observed dead leaf tissues of *N.*

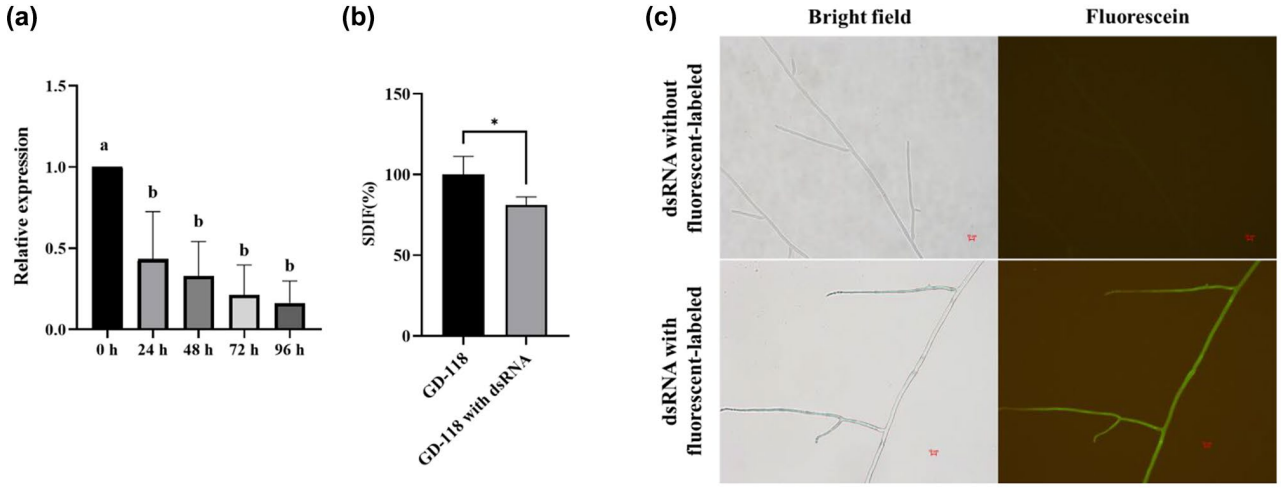

FIGURE 6 Uptake of dsRNA synthesized in vitro by hyphae of *Rhizoctonia solani* and the target gene silenced. (a) Quantitative gene expression pattern of *Rstps2* after supplementation of the dsRNA. The data were normalized to the *GAPDH* transcript levels of GD-118 and are shown as the mean ± *SE* of triplicates. Different labels represent statistical significance ($p < .05$), one-way analysis of variance and Tukey's test. (b) Sclerotial differentiation (SDIF) of sclerotia of *R. solani* AG-1 IA strain GD-118 treated with dsRNA for 10 days. Data are shown as the mean ± *SE* of triplicates. $^*p < .05$, Student's *t* test. (c) Microscopic observation of the uptake of dsRNA with fluorescently labelled dsRNA and without fluorescently labelled dsRNA of *Rstps2* by GD-118 cells

benthamiana (Figure S2b). Anderson et al. (2016) detected cell death spread on *N. benthamiana* leaves after inoculation of *R. solani*.

Conservation and evolution of pathogenicity factors across different fungal phytopathogens are some of the enigmas in the research community. It is no wonder that functions of genes involved in the fundamental processes for phytopathogenesis are conserved across fungal species/genera/families. In contrast, functions of genes that act on the determination of host range might diverge. Su et al. (2020) applied HIGS to *V. dahliae* and found 16 candidate virulence genes, including an *adenylate kinase* for which virulence function was validated in transgenic tobacco and *Arabidopsis* as well, from 92 protein-coding genes. Our candidate gene survey and HIGS assays in *N. benthamiana* revealed 29 genes that are likely to play roles in *R. solani* diseases (Figure 1). These included *AG1IA_00493*, *AG1IA_00281*, and *AG1IA_02202*, which encode homologous proteins to heat shock protein 90 in *Fusarium graminearum* (accession PHI:6272), MAP kinase in *Ustilago maydis* (accession PHI:151), and V-type proton ATPase subunit a in *Cryptococcus neoformans* (accession PHI:235), respectively. These results indicate the reliability of our HIGS system in *N. benthamiana*. In the present study, we validated the effects of *Rstps2* on virulence to *N. benthamiana* and rice. The molecular functions and mechanisms of 28 other genes remain to be characterized.

Trehalose is an essential disaccharide for the survival and virulence of pathogenic fungi and plays roles during conidiogenesis, spore germination, and sexual development (Botts et al., 2014; Cervantes-Chavez et al., 2016; Foster et al., 2003; Li et al., 2009; Puttikamonkul et al., 2010; Song et al., 2014). Trehalose protects the cells by preventing protein denaturation and scavenging ROS (Cao et al., 2008; Crowe, 2007). Thammahong et al. (2017) described two biochemical pathways for biosynthesis of trehalose in fungi: (a) synthesis from UDP-glucose by trehalose-6-phosphate synthase (Tps1) and trehalose-6-phosphate phosphatase (Tps2), and (b) synthesis from glucose-1-phosphate by trehalose phosphorylase (Thammahong et al., 2017). However, the former pathway seems to be the primary one in *R. solani* because our HIGS reduced trehalose content, and these data are based only on one transgenic line and are thus not conclusive. Nevertheless, a *Tps2* mutant in *U. maydis* resulted in a lack of trehalose production with extremely reduced virulence to maize (Cervantes-Chavez et al., 2016). Deficiency of *Tps2* in *F. graminearum* reduced virulence by 99%, while abnormal septum development and nuclear distribution in its conidia and lower mycelial growth were observed (Song et al., 2014). The results of our *Tps2* silencing experiments in GD-118 with dsRNA showed lower sclerotial dry weight. The role of trehalose in *R. solani* diseases might be the detoxification of ROS species from the host, as reported in a study on *Candida albicans* (Lu et al., 2011). Yamamoto et al. (2019) hypothesized that *R. solani* secretes a series of ROS detoxification enzymes for their pathogenicity.

We report a potential application of gene silencing of virulence factors in *R. solani* by genetic modification of crop plants. Transfer of dsRNA and siRNAs from plants to various pathogens is a common phenomenon. With no surprise, we found that *R. solani* could directly take up dsRNA from the growth environment with concomitant gene silencing over time (Figure 6). Due to the absence of completely resistant germplasm of rice against RSB (Lavale et al., 2018; Mulualem & Bekeko, 2016; Richa et al., 2017), the application of SIGS may offer an alternative crop protection approach for rice.

4 | EXPERIMENTAL PROCEDURES

4.1 | Fungal strain and plant materials

The virulent *R. solani* AG-1 IA strain GD-118 (Yang et al., 2012) was grown on PDA at 28 °C in the dark for a few days. The mycelia were

collected and used for inoculation onto tobacco/rice plants or stored at −80 °C until RNA extraction.

N. benthamiana seeds were sown on soil in pots covered with plastic films to increase humidity. Then 10-day-old *N. benthamiana* seedlings were transplanted into individual pots with soil and grown for 2 weeks at 25 °C under 55% relative humidity (RH) and a 16/8-hr light/dark period.

Seeds of a japonica rice cultivar (Nipponbare) were distributed by Wuhan Biorun Biological Technology Co., Ltd. The seeds were used for genetic transformation with RNAi constructs by the same company.

4.2 | DNA extraction, total RNA extraction, and cDNA synthesis

Genomic DNA from rice tissues was isolated using the cetyltrimethylammonium bromide method (Hormaza, 2002). Total RNA was extracted using the MiniBEST Universal RNA Extraction Kit (Takara) according to the product specifications. Approximately 2 μg of DNase-treated total RNA was used for first-strand cDNA synthesis using the Goldenstar RT6 cDNA Synthesis Kit (Beijing Tsingke Biotech Co. Ltd.) according to the manufacturer's instructions. Synthesized first-strand cDNA was stored at −20 °C for later use.

4.3 | Construction of TRV-HIGS vectors and agro-infiltration in *N. benthamiana*

Short cDNA fragments of 33 candidate genes in *R. solani* were amplified by RT-PCR using gene-specific primers with *Eco*RI and *Bam*HI linkers (Table S1). These primers were designed based on the reference genome of AG-1 IA (GenBank accession GCA_000334115.1). The resultant PCR product of each gene was digested with *Eco*RI and *Bam*HI and cloned into a linearized pTRV2 vector. A TRV2-based construct harbouring *GFP* was used as a negative control of VIGS and HIGS (Senthil-Kumar & Mysore, 2014; Su et al., 2014). A TRV2-based construct harbouring *phytoene desaturase* (*PDS*) from *N. benthamiana* (pTRV2::*PDS*) was used as a positive control for VIGS efficiency (Senthil-Kumar & Mysore, 2014). Finally, pTRV1 and these pTRV2-based constructs were separately transformed into *Agrobacterium tumefaciens* GV3101 by electroporation.

Subsequently, *Agrobacterium* cell culture of each construct was diluted to OD_{600} = 0.4 with infiltration buffer (10 mM $MgCl_2$, 10 mM MES, pH 5.6, 200 μM acetosyringone). pTRV1-transformed *Agrobacterium* cell culture was mixed in a 1:1 ratio with each pTRV2-based construct and incubated at room temperature for 4 hr. Then the mixed *Agrobacterium* solution was infiltrated into the first and second leaves of 2-week-old *N. benthamiana* using a needleless syringe. The *N. benthamiana* plants were grown at 25 °C in a growth chamber under a 16 hr light/8 hr dark photoperiod and 50% RH for at least 14 days.

4.4 | RNAi construct preparation and rice transformation

A partial cDNA fragment for *Rstps2* was amplified from the *Rstps2* cDNA by PCR with gene-specific primers that include *attB1* and *attB2* sequences in the termini and then subcloned into pDONR-221 via BP recombination with Gateway BP Clonase II (Invitrogen). The cloned *Rstps2* fragment was subcloned into two sites of a binary vector pBDL03 by LR recombination reactions with Gateway LR Clonase II (Invitrogen) (Figure S3). The T-DNA sequence of the resultant plasmid pDONR-221::*Rstps2* was verified, and the plasmid was transformed into rice via an *Agrobacterium*-mediated method by a commercial company (Wuhan Biorun Biological Technology Co., Ltd.).

Hygromycin-resistant transgenic rice lines were subjected to PCR analysis using *Rstps2*- and *hyg*-specific primers (Table S2). The positive T_0 rice lines were phenotyped by inoculation of GD-118 onto detached rice leaves. One T_0 rice line and two T_2 rice lines originating from the T_0 rice line were tested by genomic Southern blot analysis as described elsewhere (Southern, 1975). Namely, 20 μg of genomic DNA from the transgenic rice line (with increased resistance) and nontransformants was digested with *Eco*RV, and a 983-bp partial fragment of the T-DNA, which was amplified by PCR (for primers, see Table S2), was labelled with the digoxygenin DNA Labeling Kit (Roche) and used as a probe for Southern blot analysis.

4.5 | Disease phenotyping of VIGS-treated *N. benthamiana* and transgenic rice

VIGS-treated *N. benthamiana* plants were sprayed with 5 ml of *R. solani* AG-1 IA strain GD-118 mycelial suspension (OD_{600} = 1.0) and grown in an illumination incubator (90% RH, 16 hr light, 8 hr dark). After 5 days, the DI (Su et al., 2020) was measured using the following equation: DI = (no. of plants × DS score)/(total no. of plants × highest DS score × 100), where "DS score" is defined as follows: 0, no spot and no wilt; 1, less than two leaves have disease spots or wilting; 2, three or four leaves have disease spots or wilting; 3, five to seven leaves are wilting or chlorotic; and 4, plant death or near-death.

To further determine the resistance level, the third, fourth, and fifth leaves of *N. benthamiana* were selected to measure the relative lesion area using the "Lasso" tool in Adobe Photoshop CC2018 (Adobe Inc.).

To conduct disease phenotyping of transgenic rice lines at the individual plant level, one fresh sclerotium of GD-118 was inoculated on the bottom part of each tiller at the late tilling stage. The inoculated plants were then kept in a humidity chamber (RH > 90%, c.30 °C) for 5–6 days and then shifted to a normal glasshouse. At 10 days after GD-118 inoculation, the disease severity was scored by highest relative lesion height (HRLH), which was calculated as follows: HRLH = length of the highest lesion (cm)/plant height (cm) × 100% (Tiwari et al., 2017).

For disease phenotyping of detached rice leaf blades, one fresh sclerotium of GD-118 was inoculated on the centre of each detached leaf blade. Then the leaves were incubated in a humidity chamber (RH > 90%, c.30 °C) for 60 and 120 hr. The Photoshop "Lasso" tool was used to measure the percentage of the leaf area occupied by the disease area.

4.6 | RT-qPCR

qPCR was performed using a CFX96 real-time PCR system (Bio-Rad) and TransStart Top Green qPCR SuperMix (TransGen) with three biological replicates with three technical replicates. Genomic qPCR assays for the 5.8S rDNA fragment in *R. solani* AG-1 IA (GenBank accession number KX674524.1) were conducted for the estimation of fungal biomass by the method of (Tzima et al., 2012). *EF1-α* of *N. benthamiana* (GenBank accession number AF120093) and the 18S rRNA gene of rice (GenBank accession number X00755) were used as internal controls for quantitative gene expression assays (Schmidt & Delaney, 2010; Bo-Ra Kim et al., 2003). *GAPDH* (GenBank accession number ELU44274.1) was selected as the internal control of gene expression in GD-118. The relative amounts of DNA or transcripts were analysed using the $2^{-\Delta\Delta Ct}$ method (Livak & Schmittgen, 2001). The sequences of gene-specific primers used for qPCR are listed in Table S2.

4.7 | Measurement of trehalose content

Trehalose contents of GD-118 mycelia were measured using a kit (HT-2-Y) (Suzhou Comin Biotechnology Co., Ltd.) according to the manufacturer's protocol. GD-118 was reisolated from the infected rice leaves, named *Rs*-(sample). After growing on PDA for 2 days, the mycelia were collected and the trehalose content was determined. Briefly, about 0.1 g of mycelia was homogenized for the extraction of trehalose. Extracted solution (0.25 ml) was mixed with 1 ml of reaction solution and the reaction proceeded at 95 °C for 10 min. After cooling to room temperature, the absorbance (A) was recorded at 620 nm. Trehalose content was calculated as follows: trehalose content (mg/g of fresh weight) = $0.112 \times (A_{620} - 0.0729)/0.1$.

4.8 | Small RNA sequencing

GD-118 mycelia were prepared using the abovementioned method for trehalose content measurements and frozen in liquid nitrogen. The mycelia were used for small RNA sequencing by Novogene Co., Ltd. (Beijing, China). Briefly, total RNA of mycelia was extracted and used for the construction of small RNA libraries by the NEBNext Multiplex Small RNA Library Prep Set for Illumina (New England Biolabs). Short DNA fragments with a length of 140–160 bp were size-fractionated by polyacrylamide gel electrophoresis. Recovered short DNA fragments were sequenced on an Illumina HiSeq 2500 platform to generate 50-bp single-end reads.

The raw fastq files were processed by a data analysis pipeline for quality control by Novogene Co., Ltd. In this process, ambiguous sequence repeats "poly-N," the adaptor sequences, reads containing poly(A), poly(G), poly(C), and poly(T), and low-quality sequence reads were removed. Resultant high-quality short reads were mapped on the *R. solani* genome sequence by Bowtie (Langmead et al., 2009) for estimation of gene expression levels of micro-RNAs using transcript per million (TPM) values as described elsewhere (Zhou et al., 2010).

4.9 | In vitro synthesis and supplementation of fluorescently labelled dsRNA

dsRNA molecules for *Rstps2* were prepared by in vitro transcription. The partial cDNA fragment of *Rstps2* was amplified by PCR using a primer set, of which 5′ termini were linked with the T7 promoter sequence (5′-TAATACGACTCACTATAGG-3′) (Table S2). The resultant PCR products were purified using an AxyPrep PCR Clean-Up Kit (Axygen). Complementary fluorescently labelled dsRNAs were transcribed in vitro by T7 RNA polymerase (Thermo Fisher Scientific) according to the manufacturer's protocol as follows. Each 20-μl reaction solution contained 500 ng of purified PCR product, 2 μl of fluorescein RNA-labelling mix, 4 μl of transcription buffer, and 2 μl of T7 RNA polymerase. The synthesized dsRNAs were collected by ethanol precipitation.

External supplementation of dsRNA was carried out as described by McLoughlin et al. (2018). The dsRNA fraction was supplemented to GD-118 mycelia grown on potato dextrose broth (PDB) for 2 days. This incubation was conducted in 6 ml PDB with dsRNA at a final concentration of 500 ng/ml with shaking at 200 rpm at 28 °C. The mycelia were collected at 0, 24, 48, 72, and 96 hpi for gene expression analysis by RT-qPCR.

To visualize dsRNA trafficking into the hyphae of GD-118, the fungal mycelia were grown on PDA plates containing 500 ng/ml dsRNA. Cover slides were obliquely inserted into PDA, and the hyphae were visualized under an Eclipse 90i fluorescence microscope (Nikon) with elicitation of the fluorescent signals.

To determine the effect of *Rstps2* silencing on sclerotial differentiation (SDIF), GD-118 was cultured in PDA with dsRNA (500 ng/ml) or without dsRNA (control) for 10 days. Then the dry weight (DW) of mature sclerotia was determined by placing fresh sclerotia in a drying oven at 70 °C until a stable weight was reached. SDIF was calculated as follows: SDIF = $(DW)_{dsRNA} / (DW)_{control}$ (Wang et al., 2018).

ACKNOWLEDGEMENTS

This work was supported by research grants from The National Natural Science Foundation of China (no. 31801677), the Major Program of Guangdong Basic and Applied Basic Research (no. 2019B030302006), and The Research Fund Program of Guangdong Provincial Key Laboratory of New Technology in Rice Breeding (no. 2017B030314173). We thank Dr Xiaofeng Su for useful suggestions. All authors confirm that they have no conflict of interest to declare.

DATA AVAILABILITY STATEMENT

The data that support the findings of this study are available in the supplementary material of this article.

ORCID

Naoki Yamamoto https://orcid.org/0000-0002-2162-7203
Erxun Zhou https://orcid.org/0000-0003-1193-4661
Canwei Shu https://orcid.org/0000-0003-2463-4924

REFERENCES

Anderson, J.P., Hane, J.K., Stoll, T., Pain, N., Hastie, M.L., Kaur, P. et al. (2016) Proteomic analysis of *Rhizoctonia solani* identifies infection-specific, redox associated proteins and insight into adaptation to different plant hosts. *Molecular & Cellular Proteomics*, 15, 1188–1203.

Botts, M.R., Huang, M., Borchardt, R.K. & Hull, C.M. (2014) Developmental cell fate and virulence are linked to trehalose homeostasis in *Cryptococcus neoformans*. *Eukaryotic Cell*, 13, 1158–1168.

Cantarel, B.L., Coutinho, P.M., Rancurel, C., Bernard, T., Lombard, V. & Henrissat, B. (2009) The carbohydrate-active enzymes database (CAZy): an expert resource for glycogenomics. *Nucleic Acids Research*, 37, D233–D238.

Cao, Y., Wang, Y., Dai, B.D., Wang, B., Zhang, H., Zhu, Z. et al. (2008) Trehalose is an important mediator of cap1p oxidative stress response in *Candida albicans*. *Biological and Pharmaceutical Bulletin*, 31, 421–425.

Cervantes-Chávez, J.A., Valdés-Santiago, L., Bakkeren, G., Hurtado-Santiago, E., León-Ramírez, C.G., Esquivel-Naranjo, E.U. et al. (2016) Trehalose is required for stress resistance and virulence of the basidiomycota plant pathogen *Ustilago maydis*. *Microbiology*, 162, 1009–1022.

Chen, X.J., Li, L.L., He, Z., Zhang, J.H., Huang, B.L. & Chen, Z.X. et al. (2018) Molecular cloning and functional analysis of two novel polygalacturonase genes in *Rhizoctonia solani*. *Canadian Journal of Plant Pathology*, 40, 39–47.

Crowe, J.H. (2007) Trehalose as a "chemical chaperone": fact and fantasy. In: Csermely, P. & Vígh, L. (Eds.) *Advances in Experimental Medicine and Biology*, Vol. 594. New York, NY: 143–158.

Foster, A.J., Jenkinson, J.M. & Talbot, N.J. (2003) Trehalose synthesis and metabolism are required at different stages of plant infection by *Magnaporthe grisea*. *The EMBO Journal*, 22, 225–235.

Ghosh, S., Gupta, S.K. & Jha, G. (2014) Identification and functional analysis of AG1-IA specific genes of *Rhizoctonia solani*. *Current Genetics*, 60, 327–341.

Gonzalez, M., Pujol, M., Metraux, J.P., Gonzalez-Garcia, V., Bolton, M.D. & Borras-Hidalgo, O. (2011) Tobacco leaf spot and root rot caused by *Rhizoctonia solani* Kühn. *Molecular Plant Pathology*, 12, 209–216.

Govindarajulu, M., Epstein, L., Wroblewski, T. & Michelmore, R.W. (2015) Host-induced gene silencing inhibits the biotrophic pathogen causing downy mildew of lettuce. *Plant Biotechnology Journal*, 13, 875–883.

Hormaza, J.I. (2002) Molecular characterization and similarity relationships among apricot (*Prunus armeniaca* L.) genotypes using simple sequence repeats. *Theoretical and Applied Genetics*, 104, 321–328.

Kim, B.R., Nam, H.Y., Kim, S.U., Kim, S.I. & Chang, Y.J. (2003) Normalization of reverse transcription quantitative-PCR with housekeeping genes in rice. *Biotechnology Letters*, 25, 1869–1872.

Kuo, Y.W. & Falk, B.W. (2020) RNA interference approaches for plant disease control. *BioTechniques*, 69, 469–477.

Langmead, B., Trapnell, C., Pop, M. & Salzberg, S.L. (2009) Ultrafast and memory-efficient alignment of short DNA sequences to the human genome. *Genome Biology*, 10, R25.

Lavale, S.A., Prashanthi, S.K. & Fathy, K. (2018) Mapping association of molecular markers and sheath blight (*Rhizoctonia solani*) disease resistance and identification of novel resistance sources and loci in rice. *Euphytica*, 214, 78.

Li, L., Ye, Y., Pan, L., Zhu, Y., Zheng, S. & Lin, Y. (2009) The induction of trehalose and glycerol in *Saccharomyces cerevisiae* in response to various stresses. *Biochemical and Biophysical Research Communications*, 387, 778–783.

Li, S., Peng, X., Wang, Y., Hua, K., Xing, F., Zheng, Y. et al. (2019) The effector AGLIP1 in *Rhizoctonia solani* AG1 IA triggers cell death in plants and promotes disease development through inhibiting PAMP-triggered immunity in *Arabidopsis thaliana*. *Frontiers in Microbiology*, 10, 2228.

Livak, K.J. & Schmittgen, T.D. (2001) Analysis of relative gene expression data using real-time quantitative PCR and the $2^{-\Delta\Delta C(T)}$ Method. *Methods*, 25, 402–408.

Lu, H., Zhu, Z.Y., Dong, L.L., Jia, X.M., Sun, X.R. & Yan, L. (2011) Lack of trehalose accelerates H_2O_2-induced *Candida albicans* apoptosis through regulating Ca^{2+} signaling pathway and caspase activity. *PLoS One*, 6, e15808.

Mahto, B.K., Singh, A., Pareek, M., Rajam, M.V., Dhar-Ray, S. & Reddy, P.M. (2020) Host-induced silencing of the *Colletotrichum gloeosporioides conidial morphology 1* gene (*CgCOM1*) confers resistance against anthracnose disease in chilli and tomato. *Plant Molecular Biology*, 104, 381–395.

McLoughlin, A.G., Wytinck, N., Walker, P.L., Girard, I.J., Rashid, K.Y. & de Kievit, T. (2018) Identification and application of exogenous dsRNA confers plant protection against *Sclerotinia sclerotiorum* and *Botrytis cinerea*. *Scientific Reports*, 8, 7320.

Molla, K.A., Karmakar, S., Molla, J., Bajaj, P., Varshney, R.K., Datta, S.K. et al. (2020) Understanding sheath blight resistance in rice: the road behind and the road ahead. *Plant Biotechnology Journal*, 18, 895–915.

Moni, Z.R., Ali, M.A., Alam, M.S., Rahman, M.A., Bhuiyan, M.R., Mian, M.S. et al. (2016) Morphological and genetical variability among *Rhizoctonia solani* isolates causing sheath blight disease of rice. *Rice Science*, 23, 42–50.

Mulualem, T. & Bekeko, Z. (2016) Advances in quantitative trait loci, mapping and importance of markers assisted selection in plant breeding research. *International Journal of Plant Breeding and Genetics*, 10, 58–68.

Nowara, D., Gay, A., Lacomme, C., Shaw, J., Ridout, C., Douchkov, D. et al. (2010) HIGS: host-induced gene silencing in the obligate biotrophic fungal pathogen *Blumeria graminis*. *The Plant Cell*, 22, 3130–3141.

Pan, X.B., Rush, M.C., Sha, X.Y., Xie, Q.J., Linscombe, S.D., Stetina, S.R. et al. (1999) Major gene, nonallelic sheath blight resistance from the rice cultivars Jasmine 85 and Teqing. *Crop Science*, 39, 338–346.

Panwar, V., McCallum, B. & Bakkeren, G. (2013) Host-induced gene silencing of wheat leaf rust fungus *Puccinia triticina* pathogenicity genes mediated by the barley stripe mosaic virus. *Plant Molecular Biology*, 81, 595–608.

Puttikamonkul, S., Willger, S.D., Grahl, N., Perfect, J.R., Movahed, N., Bothner, B. et al. (2010) Trehalose 6-phosphate phosphatase is required for cell wall integrity and fungal virulence but not trehalose biosynthesis in the human fungal pathogen *Aspergillus fumigatus*. *Molecular Microbiology*, 77, 891–911.

Rao, T.B., Chopperla, R., Methre, R., Punniakotti, E., Venkatesh, V., Sailaja, B. et al. (2019) Pectin induced transcriptome of a *Rhizoctonia solani* strain causing sheath blight disease in rice reveals insights on key genes and RNAi machinery for development of pathogen derived resistance. *Plant Molecular Biology*, 100, 59–71.

Richa, K., Tiwari, I.M., Devanna, B.N., Botella, J.R., Sharma, V. & Sharma, T.R. (2017) Novel chitinase gene *LOC_Os11g47510* from indica rice Tetep provides enhanced resistance against sheath blight pathogen *Rhizoctonia solani* in rice. *Frontiers in Plant Science*, 8, 596.

Robertson, D. (2004) VIGS vectors for gene silencing: many targets, many tools. *Annual Review of Plant Biology*, 55, 495–519.

Sanju, S., Siddappa, S., Thakur, A., Shukla, P.K., Srivastava, N., Pattanayak, D. et al. (2015) Host-mediated gene silencing of a single effector gene from the potato pathogen *Phytophthora infestans* imparts partial resistance to late blight disease. *Functional & Integrative Genomics*, 15, 697–706.

Schmidt, G.W. & Delaney, S.K. (2010) Stable internal reference genes for normalization of real-time RT-PCR in tobacco (*Nicotiana tabacum*) during development and abiotic stress. *Molecular Genetics and Genomics*, 283, 233–241.

Senthil-Kumar, M. & Mysore, K.S. (2014) Tobacco rattle virus-based virus-induced gene silencing in *Nicotiana benthamiana*. *Nature Protocols*, 9, 1549–1562.

Shu, C., Zhao, M., Anderson, J.P., Garg, G., Singh, K.B., Zheng, W. et al. (2019) Transcriptome analysis reveals molecular mechanisms of sclerotial development in the rice sheath blight pathogen *Rhizoctonia solani* AG1-IA. *Functional & Integrative Genomics*, 19, 743–758.

Singh, P., Mazumdar, P., Harikrishna, J.A. & Babu, S. (2019) Sheath blight of rice: a review and identification of priorities for future research. *Planta*, 250, 1387–1407.

Singh, P. & Subramanian, B. (2017) Responses of rice to *Rhizoctonia solani* and its toxic metabolite in relation to expression of *Osmyb4* transcription factor. *Plant Protection Science*, 53, 208–215.

Song, X.-S., Li, H.-P., Zhang, J.-B., Song, B.o., Huang, T., Du, X.-M. et al. (2014) Trehalose 6-phosphate phosphatase is required for development, virulence and mycotoxin biosynthesis apart from trehalose biosynthesis in *Fusarium graminearum*. *Fungal Genetics and Biology*, 63, 24–41.

Song, Y. & Thomma, B.P.H.J. (2016) Host-induced gene silencing compromises Verticillium wilt in tomato and *Arabidopsis*. *Molecular Plant Pathology*, 19, 77–89.

Southern, E.M. (1975) Detection of specific sequences among DNA fragments separated by gel electrophoresis. *Journal of Molecular Biology*, 98, 503–517.

Su, X., Lu, G., Li, X., Rehman, L., Liu, W., Sun, G. et al. (2020) Host-induced gene dilencing of an adenylate kinase gene Involved in fungal energy metabolism improves plant resistance to *Verticillium dahliae*. *Biomolecules*, 10, 127.

Su, X., Qi, X. & Cheng, H. (2014) Molecular cloning and characterization of enhanced disease susceptibility 1 (*EDS1*) from *Gossypium barbadense*. *Molecular Biology Reports*, 41, 3821–3828.

Su, X., Rehman, L., Guo, H., Li, X. & Cheng, H. (2018) The oligosaccharyl transferase subunit *STT3* mediates fungal development and is required for virulence in *Verticillium dahliae*. *Current Genetics*, 64, 235–246.

Su, X., Rehman, L., Guo, H., Li, X., Zhang, R. & Cheng, H. (2017) *AAC* as a potential target gene to control *Verticillium dahliae*. *Genes*, 8, 25.

Taheri, P. & Tarighi, S. (2011) Cytomolecular aspects of rice sheath blight caused by *Rhizoctonia solani*. *European Journal of Plant Pathology*, 129, 511–528.

Thammahong, A., Puttikamonkul, S., Perfect, J.R., Brennan, R.G. & Cramer, R.A. (2017) Central role of the trehalose biosynthesis pathway in the pathogenesis of human fungal infections: opportunities and challenges for therapeutic development. *Microbiology and Molecular Biology Reviews*, 81, e00053-16.

Tiwari, I.M., Jesuraj, A., Kamboj, R., Devanna, B.N., Botella, J.R. & Sharma, T.R. (2017) Host delivered RNAi, an efficient approach to increase rice resistance to sheath blight pathogen (*Rhizoctonia solani*). *Scientific Reports*, 7, 7521.

Tzima, A.K., Paplomatas, E.J., Tsitsigiannis, D.I. & Kang, S. (2012) The G protein beta subunit controls virulence and multiple growth-and development-related traits in *Verticillium dahliae*. *Fungal Genetics and Biology*, 49, 271–283.

Urban, M., Cuzick, A., Rutherford, K., Irvine, A., Pedro, H., Pant, R. et al. (2017) PHI-base: a new interface and further additions for the multi-species pathogen-host interactions database. *Nucleic Acids Research*, 45, D604–D610.

Wang, C., Pi, L., Jiang, S., Yang, M., Shu, C. & Zhou, E. (2018) ROS and trehalose regulate sclerotial development in *Rhizoctonia solani* AG-1 IA. *Fungal Biology*, 122, 322–332.

Weiberg, A., Bellinger, M. & Jin, H. (2015) Conversations between kingdoms: small RNAs. *Current Opinion in Biotechnology*, 32, 207–215.

Yamamoto, N., Wang, Y., Lin, R., Liang, Y., Liu, Y., Zhu, J. et al. (2019) Integrative transcriptome analysis discloses the molecular basis of a heterogeneous fungal phytopathogen complex, *Rhizoctonia solani* AG-1 subgroups. *Scientific Reports*, 9, 19626.

Yang, Y.Q., Yang, M., Li, M.H., Li, Y., He, X.X. & Zhou, E.X, (2011) Establishment of *Agrobacterium tumefaciens*-mediated transformation system for rice sheath blight pathogen *Rhizoctonia solani*. *Rice Science*, 18, 297–303.

Yang, Y.Q., Yang, M., Li, M.H. & Zhou, E.X. (2012) Cloning and functional analysis of an endo-PG-encoding gene *Rrspg1* of *Rhizoctonia solani*, the causal agent of rice sheath blight. *Canadian Journal of Plant Pathology*, 34, 436–447.

Yellareddygari, S., Reddy, M., Kloepper, J., Lawrence, K. & Fadamiro, H. (2014) Rice sheath blight: a review of disease and pathogen management approaches. *Journal of Plant Pathology & Microbiology*, 5, 4.

Yin, C., Jurgenson, J.E. & Hulbert, S.H. (2011) Development of a host-induced RNAi system in the wheat stripe rust fungus *Puccinia striiformis* f. sp. *tritici*. *Molecular Plant-Microbe Interactions*, 24, 554–561.

Zhang, M., Wang, Q., Xu, K., Meng, Y., Quan, J. & Shan, W. (2011) Production of dsRNA sequences in the host plant is not sufficient to initiate gene silencing in the colonizing oomycete pathogen *Phytophthora parasitica*. *PLoS One*, 6, e28114.

Zhang, T., Jin, Y., Zhao, J.-H., Gao, F., Zhou, B.-J., Fang, Y.-Y. et al. (2016) Host-induced gene silencing of the target gene in fungal cells confers effective resistance to the cotton wilt disease pathogen *Verticillium dahliae*. *Molecular Plant*, 9, 939–942.

Zheng, A., Lin, R., Zhang, D., Qin, P., Xu, L., Ai, P. et al. (2013) The evolution and pathogenic mechanisms of the rice sheath blight pathogen. *Nature Communications*, 4, 1424.

Zhou, L., Chen, J., Li, Z., Li, X., Hu, X., Huang, Y. et al. (2010) Integrated profiling of microRNAs and mRNAs: microRNAs located on Xq27.3 associate with clear cell renal cell carcinoma. *PLoS One*, 5, e15224.

Zhu, M.H., Peng, D.D., Shu, C.W. & Zhou, E.X. (2019) Genetic diversity and pathogenicity differentiation of *Rhizoctonia solani* AG-1 IA from south China crop breeding area. *Chinese Journal of Rice Science*, 33, 176–185.

Zhu, X., Qi, T., Yang, Q., He, F., Tan, C., Ma, W. et al. (2017) Host-induced gene silencing of the MAPKK gene *PsFUZ7* confers stable resistance to wheat stripe rust. *Plant Physiology*, 175, 1853–1863.

Zou, J.H., Pan, X.B., Chen, Z.X., Xu, J.Y., Lu, J.F., Zhai, W.X. et al. (2000) Mapping quantitative trait loci controlling sheath blight resistance in two rice cultivars (*Oryza sativa* L.). *Theoretical & Applied Genetics*, 101, 569–573.

SUPPORTING INFORMATION

Additional supporting information may be found online in the Supporting Information section.

How to cite this article: Zhao, M., Wang, C., Wan, J., Li, Z., Liu, D., Yamamoto, N. et al. (2021) Functional validation of pathogenicity genes in rice sheath blight pathogen *Rhizoctonia solani* by a novel host-induced gene silencing system. *Molecular Plant Pathology*, 22, 1587–1598. https://doi.org/10.1111/mpp.13130